Rod-length dependent aggregation in a series of oligo(*p*-benzamide)-*block*-poly(ethylene glycol) rod-coil copolymers

Robert Abbel, Tobias Schleuss, Holger Frey and Andreas F.M. Kilbinger*

*Dr. A.F.M. Kilbinger
Johannes Gutenberg-Universität Mainz
Institute for Organic Chemistry
Duesbergweg 10-14
55099 Mainz
Germany
Email: akilbing@uni-mainz.de
Fax: +49 6131 3926138

Abstract

The synthesis of a series of rod-coil diblock-copolymers with flexible poly(ethylene-oxide) chains (M_n=5000 g mol^{-1}) and rod blocks consisting of monodisperse oligo(*p*-benzamide)s is described. The formation of defined supramolecular aggregates in solution as well as the solid state has been analyzed. The length of the oligo(*p*-benzamide)s has been systematically varied from n = 1-7 units. The influence of *n* on aggregation in chloroform and aqueous solution was investigated by GPC as well as UV-vis-spectroscopy. A critical aggregation length was found for chloroform (n = 5) and water (n = 4), below which no aggregation is observed under otherwise identical experimental conditions. Aggregation of the polymers in chloroform solution can be chemically reversed by the addition of PCl_5, resulting in conversion of the aromatic amides into imidoyl chlorides. Such amide-protected block-copolymers show no aggregation in NMR and GPC-experiments. Imidoyl chloride formation was shown to be reversible, i.e., addition of water regenerated the oligo(*p*-benzamide) blocks.

Keywords

diblock copolymers, oligomers, supramolecular structures, aramide, rod-coil copolymers

Introduction

Rod-coil block copolymers are an interesting class of diblock-copolymers, in which one of the blocks consists of a rigid rod-like structure, while the other consists of a flexible polymer coil. Many types of flexible linear chains as well as rod-segments and their supramolecular effect on structure formation have been studied.[1] The rod-blocks typically gain their rigidity from either conformationally fixed helix formation[2] or π-conjugation.[3] Rod-coil copolymer architectures with monodisperse oligomeric rods have also received some attention.[4-10] In such systems, the uniformity in length of the rod-segments can lead to unexpected and highly ordered superstructures in the bulk as well as in solution. Aromatic esters have mainly been used as well-defined rod segments and, therefore, most of these systems organize via relatively weak π-interactions as well as dipole interactions.

Our interest is centered on the synthesis of rod-coil block-copolymers in which the oligomeric rods possess the capability of forming strong intermolecular hydrogen bonds. Since polyaramides are known to combine chain stiffness and strong intermolecular hydrogen bonds, our objective was the preparation of block-copolymers of oligo(*p*-benzamide) (OPBA) and monomethyl poly(ethylene glycol) (MPEG). However, the preparation of the strongly aggregating, oligomeric rods is typically impeded by the insolubility of the building blocks. In a recent report we described a novel approach for the synthesis of OPBA precursors [11] (Figure 1) and their use as building blocks for rod-coil architectures. This novel route allows the preparation of OPBA-PEG block-copolymers with OPBA lengths up to the heptamer, using soluble oligomeric precursors available on the multigram scale. As the number of hydrogen bond donors and acceptors varies with the length of the rigid OPBA-rods, the attractive forces between OPBA-rods are tunable and increase with increasing OPBA length.

It is an intriguing issue in this context, to what extent the strongly aggregating OPBA-blocks influence solution and solid state properties of the block-copolymers and what role the OPBA block length plays in the supramolecular organization of these materials. In this context, it is

of particular importance to elucidate the critical aggregation length for such oligoaramide blocks. In this paper we describe both the synthesis of block-copolymers with OPBA blocks varying from monomer to heptamer and provide evidence for rod length-dependent supramolecular organization in solution and in the solid state.

Results and Discussion

Synthesis

Commercial poly(ethylene glycol) monomethyl ether (MPEG, M_n = 5000 g mol^{-1}) was functionalized with *p*-nitro benzoyl chloride to give **4** (92%) and subsequently reduced to the amine-terminated polymer MPEG-Ar_1-NH_2, (**5** 86%), as described previously (Scheme 1).[11] **5** was subsequently coupled with either *p*-nitrobenzoyl chloride, **1**, **2** or **3** (see Figure 1) yielding the polymers MPEG-Ar_m-NO_2 (m = 2-5; m represents the number of benzamide units) (**6** 81%, **7** 100%, **8** 72%, **9** 71%). Reduction of the terminal nitro groups yielded the amine-terminated polymers MPEG-Ar_m-NH_2 (m = 2-5) (**10** 50%, **11** 89%, **12** 79%, **13** 22%). **12** was further reacted with **1** or **2** to give polymers MPEG-Ar_m-NO_2 (m = 6,7) (**14** 73%, **15** 88%). The synthesis of polymers **4**, **5**, **8**, **9**, **12**, **13** and **15** has been reported previously,[11] polymers **6**, **7**, **10**, **11** and **14** were synthesized in analogy to the reported procedures. The good yields of the individual polymer analogous reactions allowed the synthesis of the final block-copolymers in multigram quantities. In the following sections we present strong evidence for the aggregation of these rod-coil block-copolymers as observed by various analytical techniques.

Aggregation in solution

Gel permeation chromatography

All polymers dissolve readily in DMF and chloroform or in water after sonification. GPC-traces of all polymers in DMF (+ 1% LiBr) show monomodal narrow molecular weight distributions. The number average molecular weight (calibrated against polystyrene standards) of the polymers increases linearly with the length of the OPBA block (Figure 2). This unambiguously shows that the polymers are molecularly dissolved and do not form aggregates in DMF. While we expected this behavior in a strongly hydrogen-bond disrupting solvent like DMF, we were interested to see the effect of a non polar solvent like chloroform on the aggregation behavior of the polymers. Therefore, GPC-experiments in chloroform of all above polymers were performed.

Chloroform solutions of polymers MPEG-Ar_m-NO_2 (m = 1-7) (**4**, **6**, **7**, **8**, **9**, **14**, **15**) were prepared and investigated by GPC. For polymers MPEG-Ar_m-NO_2 (m = 1-4) (**4**, **6**, **7**, **8**) with short OPBA-rod lengths only the molecularly dissolved species were observed in the GPC-trace, showing that the OPBA-length in these polymers was not sufficient to induce aggregation at the chosen GPC-concentrations. Polymers MPEG-Ar_m-NO_2 (m = 5-7) (**9**, **14**, **15**) with longer OPBA-rod lengths showed fundamentally different behavior. GPC-traces showed the formation of high molecular weight aggregates eluting at the separation limit of the GPC columns, as well as molecularly dissolved polymer (Figure 3). To support the non-covalent nature of the high molecular weight material, different concentrations of the polymers MPEG-Ar_m-NO_2 (m = 5-7) (**9**, **14**, **15**) were injected into the GPC-setup. In all cases, the signal intensity for the molecularly dissolved compound decreased and the signal for the high molecular weight aggregates increased with increasing concentration, confirming that the higher molecular weight species was indeed a non-covalent aggregate.

While we expected to find an OPBA rod-length dependent aggregation behavior for the block-copolymers in aqueous solution, we were surprised by the GPC-data suggesting the

existence of a critical rod length above which aggregation occurred in chloroform solution. To examine this further, we used an increased concentration of polymer MPEG-Ar_4-NO_2 (**8**) (3.5 g L^{-1}) for injection into our GPC-setup but observed only molecularly dissolved material and no aggregates. Assuming that the rod-coil block copolymers form micelles, the critical micelle concentration appears to change abruptly when extending the OPBA-rod from the tetramer to pentamer.

It is important to note that the GPC-traces of polymers MPEG-Ar_m-NO_2 (m = 5-7) (**9**, **14**, **15**) do not show aggregates of intermediate size, falling between the size of the molecularly dissolved species and the size of the high molecular weight aggregates. Hydrogen bond formation appears to play the dominant role in the supramolecular structure formation of polymers MPEG-Ar_m-NO_2 (m = 5-7) (**9**, **14**, **15**), since the stiff, rod-like shape of the aramide oligomers ensures perfect alignment for the formation of intermolecular hydrogen bonds. Aggregation most likely follows a "supramolecular step-growth mechanism" via hydrogen bond formation. We assume that aggregates with aggregation numbers below a critical value are enthalpically unfavored, which could explain the absence of aggregates of intermediate size. Investigations into the exact nature and also the visualization of the aggregates are currently being carried out.

Amine-terminated polymers MPEG-Ar_m-NH_2 (m = 2-5) (**10**-**13**) have also been examined by GPC in chloroform and DMF and showed the same behavior as the nitro-terminated polymers described above.

UV-vis and Fluorescence spectroscopy

It is well-known that aggregation of chromophores can result in shifts of the absorption maximum in UV-vis spectra as well as quenching of the fluorescence intensity.[12] As shown previously, unsubstituted OPBAs up to the tetramer show a red shift of the absorption maximum with increasing oligomer length[11], indicating partial conjugation across the

aromatic amide bond. The series of extended OPBAs up to the heptamer as present in the block copolymers in this study was therefore expected to be a useful set of compounds for a UV-vis spectroscopic investigation of aggregation behavior.

In order to be able to compare the spectroscopic data to the results obtained from the GPC-experiments, we recorded UV-vis and fluorescence spectra of polymers MPEG-Ar_m-NH_2 (m = 2-5) (**10**-**13**) in chloroform and DMF. The amine terminated polymers generally show higher fluorescence intensities than the nitro-terminated polymers and are therefore reported here, although the general trend was the same in both series of compounds.

As expected, the absorption maximum of the amine-terminated oligoaramide block copolymers in DMF increases with increasing OPBA length (Figure 4). A linear relationship is observed between the wavelength of the absorption maximum and the inverse of the oligomer length 1/n. This is indicative of molecular solvation of the OPBA rods and correlates well with the observations from GPC-measurements in the same solvent.

The increase in absorption coefficient and decrease in fluorescence intensity with increasing oligomer length is typical for extended π-conjugated oligomers that show some degree of conformational freedom.

In order to investigate whether the aggregation phenomena observed in chloroform effect the photo-physical properties of the block-copolymers, we recorded UV-vis and fluorescence spectra of the amine-terminated oligoaramide block copolymers MPEG-Ar_m-NH_2 (m = 2-5) (**10**-**13**) in chloroform (Figure 5). The wavelength of the absorption maximum shifts to longer wavelengths with increasing OPBA length up to an oligomer length of m = 4. For m = 5 a blue shift of $\Delta\lambda$ = 25 nm (from m = 4 to m = 5) is observed, indicating parallel stacking of the OPBA chromophores (H-aggregate).[12] This abrupt change in absorption maximum from OPBA oligomers with m = 4 to m = 5 matches exactly the onset of aggregation observed in chloroform GPC-experiments. Compared to the spectra in DMF, the fluorescence spectra in chloroform are significantly reduced in intensity. Two emission bands can be observed, the

one at longer wavelength increases in intensity with increasing OPBA length up to m = 4. For m = 5 the emission band at longer wavelength is markedly reduced in intensity. We ascribe this to the onset of aggregation of OPBA chromophores.

To maximize the difference in solvent quality for the two blocks, we chose water which is a good solvent for the PEG block but a non-solvent for the OPBA block. UV-vis and fluorescence spectra recorded for polymers MPEG-Ar_m-NH_2 (m = 2-5) (**10-13**) in water are shown in Figure 6.

Similar to the UV-vis spectra in chloroform an abrupt blue shift can be observed when increasing the OPBA block length from m = 3 to m = 4. Clearly, in water the onset of aggregation occurs at shorter OPBA rod lengths (m = 4) compared to chloroform (m = 5), reflecting the fact that water is a poorer solvent for the OPBA rods than chloroform. As expected for highly polar solvents like water, the fluorescence of the OPBA rods is quenched.

Interaction of the polybenzamide-blocks in the solid state

Based on these observations, it is intriguing, whether the strong intermolecular forces of the short OPBA blocks that are responsible for supramolecular structure formation in solution influence the physical properties of the PEG-block in the solid state. Thus, block-copolymers MPEG-Ar_m-NH_2 (m=1-5) (m=1 **5**, m=2 **10**, m=3 **11**, m=4 **12**, m=5 **13**) as well as the unmodified MPEG-OH were thermally characterized by differential scanning calorimetry (DSC) (-100°C to +140°C, heating rate = 10 °C min^{-1}). As can be seen in Figure 7, the melt enthalpy of the PEG segments in these block-copolymers decreases linearly with increasing length *m* of the OPBA-block, while the onset temperature of the melting of the PEG blocks remains constant. This can be explained by phase segregated crystalline domains of OPBA. The crystallization of the OPBA-rods impedes crystallization of the PEG segments in the vicinity of the OPBA domains, which, in turn leads to the observation of a reduced melt enthalpy in the DSC measurement. For block-copolymers with OPBA-rod segments equal or

longer than the hexamer, a glass transition is also observed in the DSC trace (see Figure 8 as an example). This is due to an increasing amorphous fraction of PEG surrounding the OPBA-rod domains. These experiments clearly show that relatively short OPBA rods have a pronounced influence on the solid state properties of the block copolymers. Detailed structural studies concerning the packing of both blocks are currently in progress.

De-aggregation through chemical reaction

Many examples of the conversion of low molecular weight amides to imidoyl chlorides have been reported in the literature. One reagent that is commonly used and reacts with aromatic amides at room temperature is PCl_5.[13] One of the objectives of this study was to establish whether the aggregation behavior observed for OPBA-PEG block copolymers in chloroform, which we attributed to hydrogen bond formation, could be reversed by protecting the aromatic amides with a suitable protecting group, i.e. by transforming them into imidoyl chlorides in a polymer-analogous reaction. With this in mind, we recorded a ^{1}H-NMR spectrum of polymer MPEG-Ar_7-NO_2 (**15**) in chloroform-d. Polymer MPEG-Ar_7-NO_2 (**15**) was selected, as it showed the strongest aggregation in chloroform in previous GPC-experiments. As expected, no signals for the aromatic protons could be discerned in the ^{1}H-NMR-spectrum (Figure 9, bottom) due to signal broadening. A 10-fold excess of PCl_5 was then added to the solution at room temperature and the ^{1}H-NMR-spectrum recorded again after stirring for 12h (Figure 9, top). The presence of sharp signals for aromatic protons (δ = 6.8-8.5 ppm) as well as the appearance of two sets of methylene protons in the vicinity of the ester function (δ = 4.4 and 3.8 ppm), together with the absence of amide N-H-signals (δ = 10.0-11.0 ppm), evidence that quantitative imidoyl chloride formation had indeed taken place and that the OPBA rod was still attached to the polymer chain. As expected, the new block-copolymer did not appear to form aggregates in chloroform.

To obtain additional evidence for this transformation and its supramolecular consequences, a GPC-trace of the above chloroform solution was recorded and compared to the trace obtained for unmodified polymer MPEG-Ar_7-NO_2 (**15**) (Figure 10). The broad peak for the aggregated polymer which accounted for most of the signal intensity in the trace of the unmodified sample had completely disappeared in the PCl_5-treated polymer sample. This clearly shows that the main driving force for aggregation is hydrogen bond formation, and π-stacking is negligible in the case of these short aramide oligomers. To show the reversibility of the protection process, a sample of PCl_5 treated polymer **15** was exposed to moisture for 12h. The ^{1}H-NMR spectrum of the sample as well as the GPC-trace showed the aggregated form of the initial polymer. Thus, the imidoyl-chloride formation represents an interesting precursor route for processing of the materials, e.g., in thin films or fibers.

Another important facette of imidoyl chloride formation was revealed in mass spectroscopy experiments. All attempts to characterize the block copolymer MPEG-Ar_7-NO_2 (**15**) via MALDI-TOF spectroscopy failed, most likely due to the strong interaction of the OPBA-blocks of the copolymer in the solid state. However, after treatment of a chloroform solution of MPEG-Ar_7-NO_2 (**15**) with PCl_5 the oligo aramide block was protected as the non-aggregating imidoyl chloride form. In this case the materials could be characterized by MALDI-TOF under conditions which previously gave no product signals for unmodified polymer **15** (Figure 11). The MALDI-TOF spectrum supports both quantitative attachment as well as the monodisperse character of the OPBA-segments. The polydispersity observed is merely due to the PEG-block.

Conclusion

We have shown that the previously described OPBA precursors are valuable building blocks for the synthesis of PEG-OPBA-rod-coil block-copolymers. Copolymers with oligoaramide block lengths up to the heptamer have been prepared and investigated with regard to their OPBA block length-dependent aggregation behavior in solution and in the solid state. For further supramolecular applications of OPBAs, it is of crucial importance to know the degree of polymerization required for aggregation. This critical rod length was obtained for the pentamer in order to show aggregation in a chloroform GPC-setup in the concentration range ($c = 0.5\text{-}3.5\ gL^{-1}$). The rod-length dependent aggregation behavior can be correlated to UV-vis spectra of the copolymers, which show an abrupt blue-shift of the absorption maximum from tetramer to pentamer. UV-vis spectra of the polymers in water show a similar blue-shift for the transition OPBA-trimer/tetramer-PEG-block copolymers. DSC measurements of the block-copolymers with OPBA rod lengths exceeding n=6 show a glass transition temperature for the PEG-block at T = -65°C.

The supramolecular aggregation of the OPBA-heptamer-block-copolymer in chloroform can be chemically reversed by simple addition of PCl_5 to the polymer solution. ^{1}H-NMR as well as GPC-experiments confirmed the de-aggregation process. In analogy to the synthesis of OPBA precursors, the aromatic amides in the block-copolymer are converted into imidoyl chlorides which cannot aggregate via hydrogen-bonds. This reversible polymer analogous de-aggregation route opens possibilities for numerous applications, like coatings or polymer blends, in which a molecularly dissolved precursor form of the polymer is required. Micellar structures observed for the block-copolymers are currently investigated and visualized via AFM and TEM as well as light scattering.

Experimental Section

General: Technical grade solvents were purchased from Acros Organics, those of analytical quality (p. a. grade) were purchased from Fisher Scientific. Dichloromethane was dried over P_4O_{10} , distilled and stored over molecular sieves (4 Å). Chloroform was vacuum distilled before use. Deuterated solvents were purchased from Deutero GmbH. All poly(ethylene glycol)s were purchased from Fluka, all other reagents from Acros Organics and used without further purification.

Standard ^{1}H nuclear magnetic resonance spectra were recorded at 300 MHz on a Bruker AC 300. ^{1}H-NMR-signals due to protons of the poly(ethylene glycol) chain are not reported.

UV-VIS spectra were recorded on a Shimadzu UV-210 2 PC scanning spectrophotometer.

Fluorescence spectra were measured on a Spex Fluorolog 2 with photomultiplier tube.

DSC curves were recorded on a Perkin Elmer DSC 7 and a Perkin Elmer Thermal Analysis Controler TAC 7/DX.

Gel permeation chromatography with chloroform was performed on an instrument consisting of a Waters 717 plus auto sampler, a TSP Spectra Series P 100 pump and a set of three PSS SDV columns ($10^6/10^5/10^4$ g/mol for high molecular masses, $10^4/10^3/10^2$ g/mol for low molecular masses g/mol). Signal detection occurred by use of a TSP Spectra System UV 2000 (UV 254 nm) and a Wyatt Optilab DSP (refractive index). For measurements in DMF containing 1 g/L of lithium bromide, an Agilent 1100 Series was used as an integrated instrument including a PSS Gral column ($10^6/10^5/10^4$ g/mol), a UV (254 nm) and RI detector. Calibration was done using poly(styrene) standards provided by Polymer Standards Service.

MALDI-TOF mass spectra were recorded on a Kratos Axima CFR in linear mode using dithranol as matrix.

The synthesis of compounds **1-5**, **8**, **9**, **12**, **13** and **15** has been described previously.[11] Compounds **6**, **7**, **10**, **11** and **14** were prepared in analogy to the previously reported procedures. Only analytical data of these compounds is reported here.

MeO-PEG(5k)-Ar$_2$-NO$_2$ (6): 2 g of **5** gave 1.61 g of **6** (81 %).

^{1}H-NMR (DMSO-d$_6$): δ 7.93 – 8.00 (m), 8.19 (d, 8.8 Hz), 8.37 (d, 8.8 Hz), 10.86 (s). IR: $\tilde{\nu}$ = 2880 (CH$_2$), 1679 (C=O), 1529 (NO$_2$) cm^{-1}. GPC (DMF + 1 g/L LiBr): M_n = 7980, M_w = 8330 g/mol, PDI = 1.03 (UV); M_n = 8310, M_w = 8600 g/mol, PDI = 1.03 (RI).

MeO-PEG(5k)-Ar$_3$-NO$_2$ (7): 3 g of **5** gave 3.03 g of **7** (quant.).

^{1}H-NMR (DMSO-d$_6$): δ 7.95 – 8.05 (m), 8.21 (d, 8.8 Hz), 8.39 (d, 8.8 Hz), 10.48 (s), 10.82 (s). IR: $\tilde{\nu}$ = 2884 (CH$_2$), 1677 (C=O), 1529 (NO$_2$) cm^{-1}. GPC (DMF + 1 g/L LiBr): M_n = 8410, M_w = 8830 g/mol, PDI = 1.05 (UV); M_n = 8500, M_w = 8930 g/mol PDI = 1.03 (RI).

MeO-PEG(5k)-Ar$_2$-NH$_2$ (10): 1 g of **6** gave 500 mg of **10** (50 %) after reduction with 1 g of formate and 50 mg Pd/C (10 %).

^{1}H-NMR (DMSO-d$_6$): δ 5.81 (s), 6.59 (d, 8.8 Hz), 7.72 (d, 8.8 Hz), 7.90 – 8.03 (m), 10.05 (s). IR: $\tilde{\nu}$ = 3351 (NH), 2880 (CH$_2$), 1605 (NH$_2$) cm^{-1}. GPC (DMF + 1 g/L LiBr): M_n = 8120, M_w = 8420 g/mol, PDI = 1.04 (UV); M_n = 8120, M_w = 8400 g/mol, PDI = 1.04 (RI).

MeO-PEG(5k)-Ar$_3$-NH$_2$ (11): 2.25 g of **7** gave 2 g of **11** (89 %) after reduction with 2.8 g of formate and 300 mg Pd/C (10 %).

^{1}H-NMR (DMSO-d$_6$): δ 5.80 (s), 6.60 (d, 8.8 Hz), 7.75 (d, 8.8 Hz), 7.95 – 8.05 (m), 10.02 (s), 10.41 (s). IR: $\tilde{\nu}$ = 3338 (NH), 2882 (CH$_2$), 1669 (C=O), 1604 (NH$_2$) cm^{-1}. GPC (DMF + 1 g/L LiBr): M_n = 8440, M_w = 8700 g/mol, PDI = 1.03 (UV); M_n = 8430, M_w = 8670 g/mol, PDI = 1.03 (RI).

MeO-PEG(5k)-Ar$_6$-NO$_2$ (14): 1.5 g of **12** and 0.5 g of **1** gave 1.1 g of **14** (73 %) ^{1}H-NMR (DMSO-d$_6$): δ 7.95 – 8.05 (m), 8.22 (d, 8.8 Hz), 8.39 (d, 8.8 Hz), 10.44 (s), 10.48 (s), 10.85 (s). IR: $\tilde{\nu}$ = 3342 (NH), 2882 (CH$_2$), 1658 (C=O), 1524 (NO$_2$) cm^{-1} GPC (DMF + 1 g/L LiBr): M_n = 9860, M_w = 10220 g/mol, PDI = 1.04 (UV); M_n = 9800, M_w = 10220 g/mol, PDI = 1.04 (RI).

Reaction of 15 with PCl$_5$:

Copolymer **15** (150 mg, 0.026 mmol) were dissolved in CDCl$_3$ (1.5 ml) and PCl$_5$ (80 mg, 0.3 mmol) added at r.t. for 12h.

Acknowledgements

AFMK thanks E. Berger-Nicoletti for MALDI-TOF characterizations and the Fonds der Chemischen Industrie (FCI) for funding.

References

[1] Lee, M.; Cho, B.-K.; Zin, W.-C. *Chem. Rev.* **2001**, *101*, 3869.

[2] see for example: Vriezema, D. M.; Kros, A.; de Gelder, R.; Cornelissen, J. J. L. M.; Rowan, A. E.; Nolte, R. J. M. *Macromolecules* **2004**, *37*, 4736; Park, J.-W.; Thomas, E. L. *Macromolecules* **2004**, *37*, 3532; Schlaad, H.; Smarsly, B.; Losik, M. *Macromolecules* **2004**, *37*, 2210.

[3] for a recent example see Lee, M.; Jang, C.J.; Ryu, J.H. *J. Am. Chem. Soc.* **2004**, *126*, 8082.

[4] Lee, M.; Park, M.-H.; Oh, N.-K.; Zin, W.-C.; Jung, H.-T.; Yoon, D. K. *Angew. Chem.*, **2004**, *116*, 6628.

[5] Lee, M.; Jang, C.-J.; Ryu, J.-H. *J. Am. Chem. Soc*. **2004**, *126*, 8082.

[6] Chochos, C. L.; Tsolakis, P. K.; Gregoriou, V. G.; Kallitsis, J. K. *Macromolecules* **2004**, *37*, 2502.

[7] Ryu, J.-H.; Oh, N.-K.; Zin, W.-C.; Lee, M. *J. Am. Chem. Soc*. **2004**, *126*, 3551.

[8] Gopalan, P.; Li, X.; Li, M.; Ober, C. K.; Gonzales, C. P.; Hawker, C. J. *J. Polym. Sci. A* **2003**, *41*, 3640.

[9] Radzilowski, L. H.; Wu, J. L.; Stupp, S. I. *Macromolecules*, **1993**, *26*, 879.

[10] Radzilowski, L. H.; Carragher, C.O.; Stupp, S.I. *Macromolecules* **1997**, *30*, 2110.

[11] Abbel, R.; Frey, H.; Schollmeyer, D.; Kilbinger, A. F. M. *Chem. Eur. J*. **2005**, *11*, 2170.

[12] Pope, M.; Swenberg, C. E. "Electronic Processes in Organic Crystals and Polymers", 2nd Edition, Oxford University Press, **1999**, Oxford.

[13] see for example: Ruane, P. H.; Ahmed, A. R.; McClelland, R. A. *J. Chem. Soc. Perkin Trans.2*, **2002**, *2*, 312; Schenck, T. G.; Bosnich, B.; *J. Amer. Chem .Soc*. **1985**, *107*, 2058.

Captions of all Figures and Schemes

Figure 1. OPBA precursors as described previously.[11]

Scheme 1. Synthetic scheme for the preparation of OPBA-MPEG rod-coil block-copolymers. i) triethyl amine, ii) ammonium formate, Pd/C, iii) *p*-nitrobenzoyl chloride, **1**, **2** or **3**, N,N-dimethyl aniline iv) ammonium formate, Pd/C, v) **1** or **2,** N,N-dimethyl aniline.

Figure 2. GPC-traces (DMF) of MPEG-Ar_m-NO_2 show a linear relationship between M_n (calibrated with PS standards) and OPBA length *n* (m=1 **4**, m=2 **6**, m=3 **7**, m=4 **8**, m=5 **9**, m=6 **14**, m=7 **15**).

Figure 3. GPC-traces of MPEG-Ar_m-NO_2 in Chloroform (0.5 g L^{-1}). m=4 (**8**), m=5 (**9**), m=7 (**15**).

Figure 4. UV-vis and fluorescence spectra of MPEG-Ar_m-NH_2, m=2-5 in DMF ($7.8 \cdot 10^{-6}$ mol L^{-1}): m=2 (**10**), m=3 (**11**), m=4 (**12**), m=5 (**13**).

Figure 5. UV-vis and fluorescence spectra of MPEG-Ar_m-NH_2, m=1-5 in $CHCl_3$ ($7.8 \cdot 10^{-6}$ mol L^{-1}) : m=2 (**10**), m=3 (**11**), m=4 (**12**), m=5 (**13**).

Figure 6. UV-vis and fluorescence spectra of MPEG-Ar_m-NH_2, m=2-5 in H_2O ($7.8 \cdot 10^{-6}$ mol L^{-1}) : m=2 (**10**), m=3 (**11**), m=4 (**12**), m=5 (**13**).

Figure 7. DSC data for MPEG-Ar_m-NH_2 (m=1 **5**, m=2 **10**, m=3 **11**, m=4 **12**, m=5 **13**, m=0 unmodified MPEG). Triangles: melt enthalpy of the PEG segment (corrected for the different mass percentages of PEG present in the copolymers), squares: onset of the PEG-segment melt transition.

Figure 8. DSC trace for MPEG-Ar_7-NO_2 (**15**) showing a glass transition at T_g = -65°C and a melt transition at T_m = 56 °C (heating rate = 10°C min^{-1}).

Figure 9. ^{1}H-NMR spectra of polymer **15** in $CDCl_3$. Bottom: without additives, top: with PCl_5 added to the solution.

Figure 10. GPC-traces for polymer **15**. Solid line: modified with PCl_5, dashed line: unmodified. (c = 0.5 g L^{-1}).

Figure 11. MALDI-TOF spectrum of polymer **15** treated with PCl_5.

Figures and Schemes

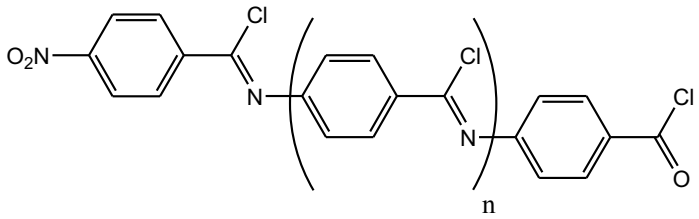

n = 0: **1**
1: **2**
2: **3**

Figure 1. OPBA precursors, as described previously.[11]

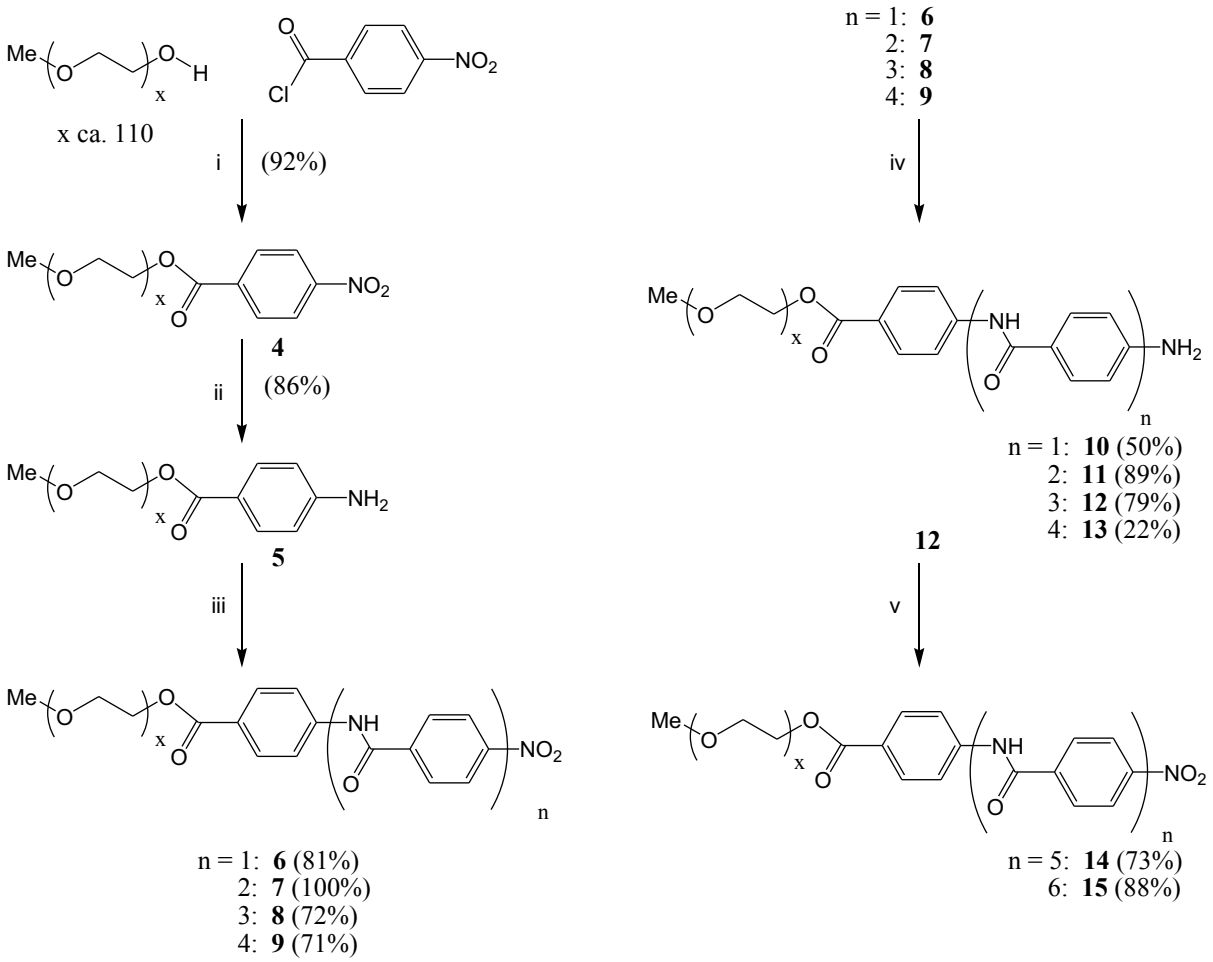

Scheme 1. Synthetic scheme for the preparation of OPBA-MPEG rod-coil block-copolymers. i) triethyl amine, ii) ammonium formate, Pd/C, iii) *p*-nitrobenzoyl chloride, **1**, **2** or **3**, N,N-dimethyl aniline iv) ammonium formate, Pd/C, v) **1** or **2,** N,N-dimethyl aniline.

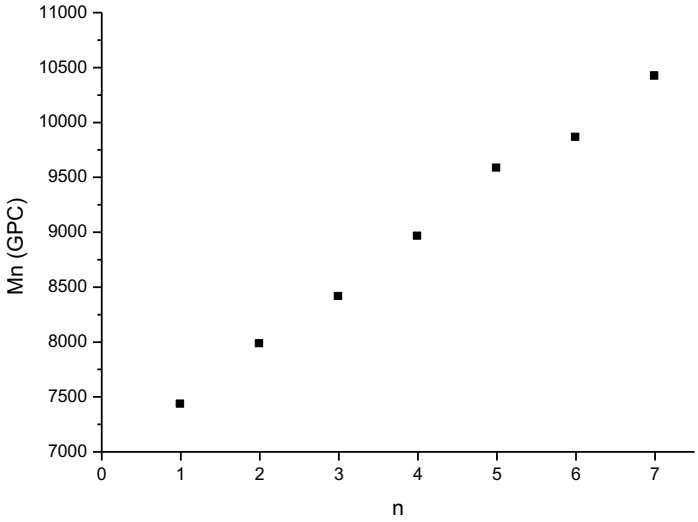

Figure 2. GPC-traces (DMF) of MPEG-Ar_n-NO_2 show a linear relationship between M_n (calibrated with PS standards) and OPBA length *m* (m=1 **4**, m=2 **6**, m=3 **7**, m=4 **8**, m=5 **9**, m=6 **14**, m=7 **15**).

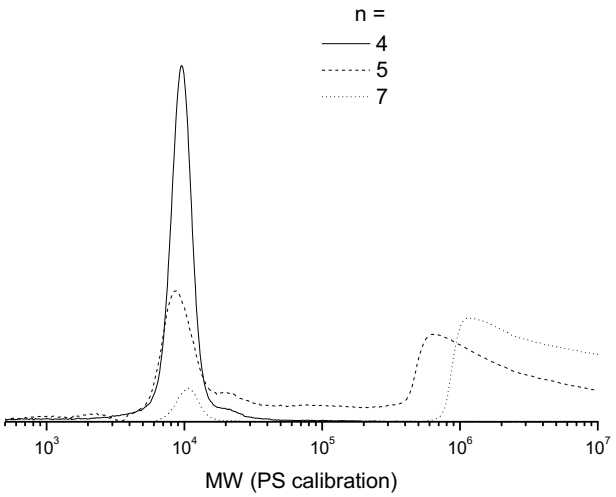

Figure 3. GPC-traces of MPEG-Ar_m-NO_2 in Chloroform (0.5 g L^{-1}). m=4 (**8**), m=5 (**9**), m=7 (**15**).

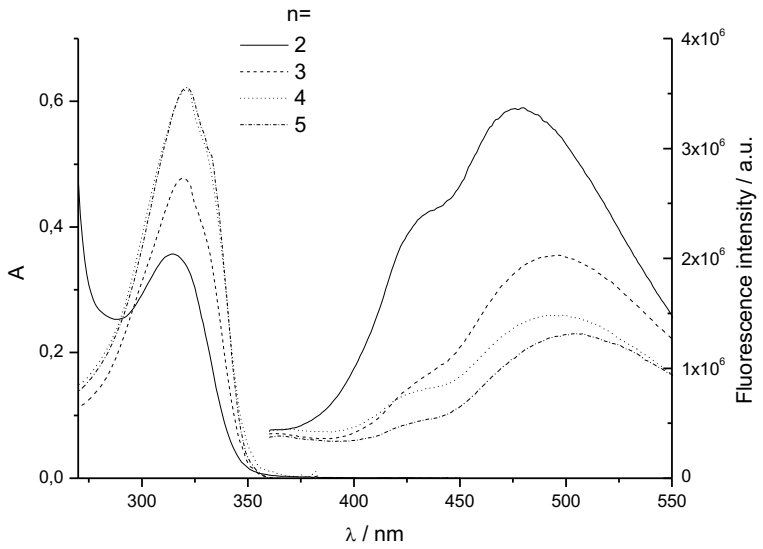

Figure 4. UV-vis and fluorescence spectra of MPEG-Ar_m-NH_2, m=2-5 in DMF ($7.8 \cdot 10^{-6}$ mol L^{-1}): m=2 (**10**), m=3 (**11**), m=4 (**12**), m=5 (**13**).

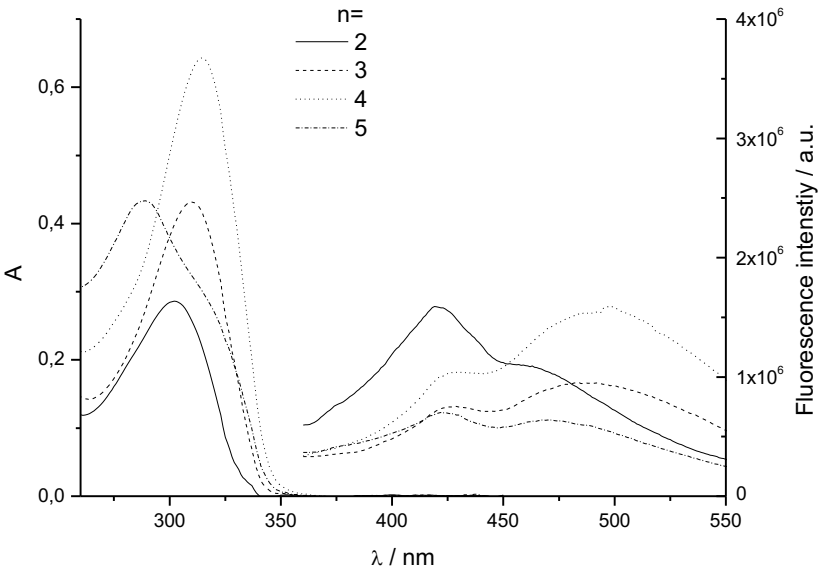

Figure 5. UV-vis and fluorescence spectra of MPEG-Ar_m-NH_2, m=1-5 in $CHCl_3$ ($7.8 \cdot 10^{-6}$ mol L^{-1}) : m=2 (**10**), m=3 (**11**), m=4 (**12**), m=5 (**13**).

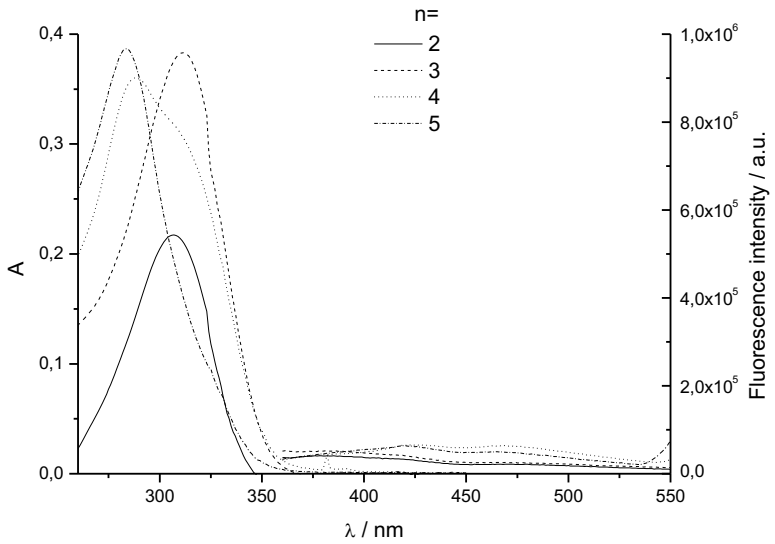

Figure 6. UV-vis and fluorescence spectra of MPEG-Ar_m-NH_2, m=2-5 in H_2O ($7.8 \cdot 10^{-6}$ mol L^{-1}) : m=2 (**10**), m=3 (**11**), m=4 (**12**), m=5 (**13**).

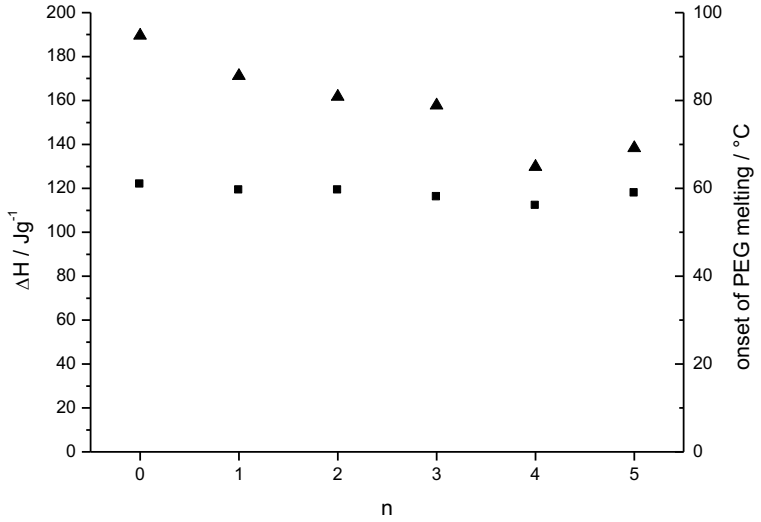

Figure 7. DSC data for MPEG-Ar_m-NH_2 (m=1 **5**, m=2 **10**, m=3 **11**, m=4 **12**, m=5 **13**, m=0 unmodified MPEG). Triangles: melt enthalpy of the PEG segment (corrected for the different mass percentages of PEG present in the copolymers), squares: onset of the PEG-segment melt transition.

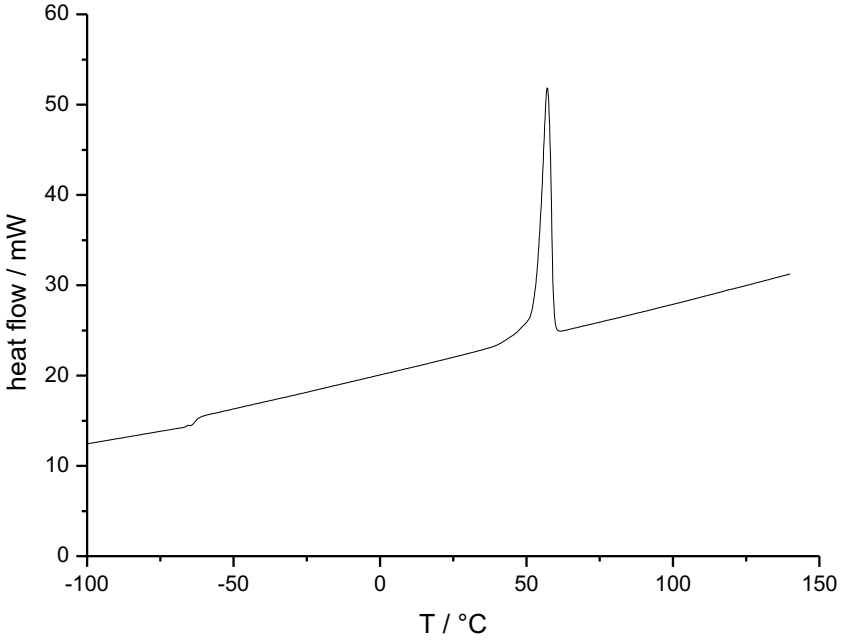

Figure 8. DSC trace for MPEG-Ar_7-NO_2 (**15**) showing a glass transition at T_g = -65°C and a melt transition at T_m = 56 °C (heating rate = 10°C min^{-1}).

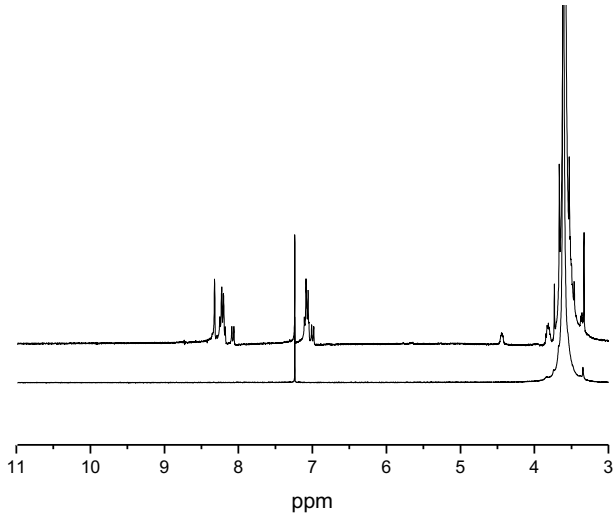

Figure 9. ^{1}H-NMR spectra of polymer **15** in $CDCl_3$. Bottom: without additives, top: with PCl_5 added to the solution. Both ^{1}H-NMR spectra are arranged such that the peaks of residual protonated chloroform (δ = 7.26 ppm) appear as one peak.

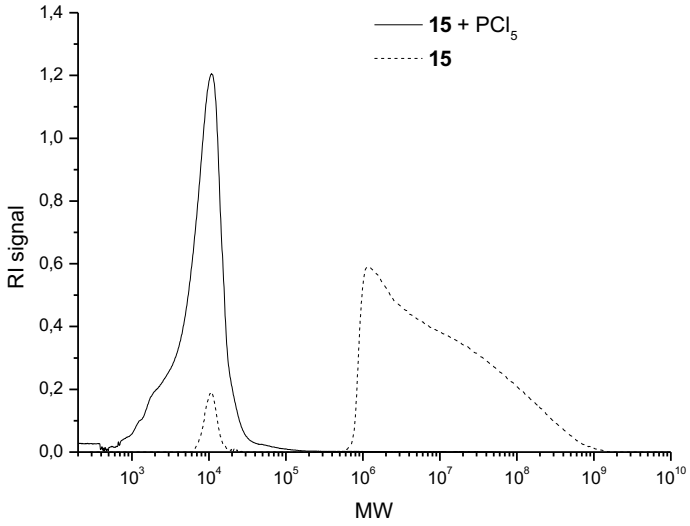

Figure 10. GPC-traces for polymer **15**. Solid line: modified with PCl_5, dashed line: unmodified. ($c = 0.5$ g L^{-1}).

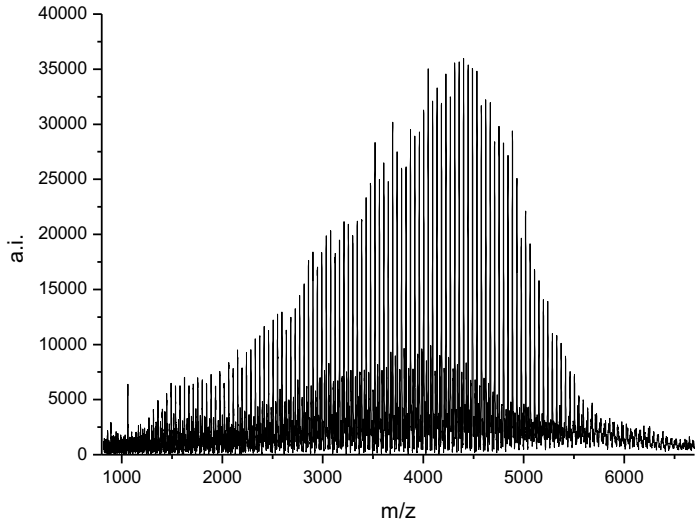

Figure 11. MALDI-TOF spectrum of polymer **15** treated with PCl_5.

Text for the table of contents

Poly(ethylene glycol)-*co*-oligo(p-benzamide)s with exactly defined oligoaramide blocks have been synthesized and their solution organization investigated in polar and non-polar solvents. In chloroform-d the aggregated form of the aramide block copolymer can be reversible turned into the molecularly dissolved form via polymer analogous formation of imidoyl chlorides using PCl_5.

Graphical abstract